

Original Article

## Characterization of Surface Morphology and Magnetic Properties of Fe<sub>3</sub>O<sub>4</sub>-Deposited Alginate Bead



Swee Pin Yeap<sup>\*</sup>, Mohammad Afiq Afiki Bin Ismail

Department of Chemical and Petroleum Engineering, Faculty of Engineering, Technology, and Built Environment, UCSI University, 56000, Cheras, Kuala Lumpur, Malaysia.

### Abstract

It is generally known that Fe<sub>3</sub>O<sub>4</sub> nanoparticles are magnetically separable and thus, have been widely used in water treatment. However, magnetophoresis of the singly dispersed Fe<sub>3</sub>O<sub>4</sub> nanoparticles has been proven to be slow. Realizing this limitation, the present work aims to immobilise various quantities of nano-Fe<sub>3</sub>O<sub>4</sub> onto the surface of an alginate bead to promote cooperative magnetophoresis. The formed nano-Fe<sub>3</sub>O<sub>4</sub> deposited alginate beads were characterized for their surface morphology and magnetic properties using scanning electron microscopy (SEM) and vibrating sample magnetometry (VSM), respectively. SEM analysis showed that the external surface of the alginate bead turns porous upon subjecting to sonication process. The pores serve as the template to hold the Fe<sub>3</sub>O<sub>4</sub> nanoparticles in place. Upon the deposition of Fe<sub>3</sub>O<sub>4</sub> nanoparticles, the external surface of alginate bead turned rougher. Besides changes in surface morphology, the saturation magnetization value of the beads recorded a substantial increment along with the loading amount of Fe<sub>3</sub>O<sub>4</sub>. Such observation proved that it is feasible to induce a cooperative magnetic effect by immobilise various quantities of Fe<sub>3</sub>O<sub>4</sub> onto the surface of alginate bead.

Copyright © 2020 PENERBIT AKADEMIA BARU - All rights reserved

### Article Info

Received 24 April 2020

Received in revised form 20 May 2020

Accepted 21 May 2020

Available online 22 May 2020

### Keywords

Magnetic nanoparticles  
Alginate bead  
Surface deposition  
Saturation magnetization  
Surface morphology

## 1 Introduction

Nanotechnology has been the key technology to combat many environmental issues especially in water and wastewater treatment [1,2]. In specific, nanoparticles are the particles with at least one of the dimensions fall within the nanoscale range (1 nm to 100 nm). Each type of nanoparticles has their own unique properties. Out of the many types of nanoparticles, magnetic nanoparticles have received great interest for water treatment owing to their ability to respond to magnetic field. Accordingly, these nanoparticles offer an advantage whereby they can be easily separated after their applications. Nevertheless, collecting magnetic nanoparticles from a large volume of liquid medium can be challenging. In fact, the magnetophoresis rate can be rather slow if the magnetic nanoparticles move individually or as a tiny cluster [3,4]. The time lag poses a serious challenge for the effective use of magnetic nanoparticles in water treatment [5]. Hence, it was proposed to attach an amount of magnetic nanoparticles onto other substrates (such as microcapsule [6], activated carbon [7], biomass [8,9]) in order to fully realise its feasibility for water treatment.

Nevertheless, some of the substrates require the use of high temperature, pressure, or toxic chemical for preparation. For instance, synthesis of activated carbon involves high temperature pyrolysis process

<sup>\*</sup> Corresponding author yeapsw@ucsiuniversity.edu.my ✉

(300 – 900°C) [10,11]. In this work, alginate bead, a more environmentally friendly material made from bio-resources (seaweed), was used as the substrate to hold the nanoparticles. The production of alginate bead is simple, does not require any hazardous material, solvent or special conditions; thus, it is preferable for large scale industrial application. In fact, alginate-based composites have been widely employed as an adsorbent for pollutant removal [12,13]. Noteworthy that the physical characteristics of an adsorbent are associated with its application performance [14]. Thus, besides to deposit magnetic nanoparticles onto the external surface of an alginate bead, the present work also aims to characterize its surface and magnetic properties.

## 2 Methodology and Experiment Setup

### 2.1 Preparation of Alginate Beads

Alginate bead was prepared from the gelation of sodium alginate using calcium chloride as the crosslinking agent [15]. Both chemicals were obtained from Chemiz. First, sodium alginate powder weighted 2 g was dissolved in 100 mL of distilled water to give an alginate solution of 2 wt% concentration. The mixture was stirred at 80°C until a transparent and viscous solution was obtained. After that, the solution was added drop-by-drop into a continuously stirred calcium chloride solution in which the alginate gel beads were formed. The formed alginate beads were then rinsed with distilled water to remove excess reactant.

### 2.2 Depositing Nano-Fe<sub>3</sub>O<sub>4</sub> onto the Surface of Alginate Beads

0.25 g/L of Fe<sub>3</sub>O<sub>4</sub> nanoparticle suspension was prepared by dispersing Fe<sub>3</sub>O<sub>4</sub> nanopowder (Nanoamor, USA) into distilled water. The suspension was subjected to 1-hour of ultrasonication using a sonicator bath. Then, alginate beads were poured into the suspension and followed by another 1-hour of ultrasonication. The second round of sonication was to reduce the extent of particle agglomeration as well as to enhance the mixing of nanoparticles with the bead. It was expected that the nanoparticles will deposit on the external surface of the alginate bead, as illustrated in Fig. 1. The nano-Fe<sub>3</sub>O<sub>4</sub> deposited alginate beads were then rinsed several times with distilled water to remove any unbound or loosely bound nanoparticles. Similar procedures were repeated by increase the amount of Fe<sub>3</sub>O<sub>4</sub> loading from 0.25 g/L to 3.0 g/L. As shown in Fig. 2, the nano-Fe<sub>3</sub>O<sub>4</sub> deposited alginate beads appear to be brownish in colour, indicating successful attachment of Fe<sub>3</sub>O<sub>4</sub> nanoparticles onto the bead. The beads were air-dried (instead of oven-dried to avoid extreme shrinkage) before proceeding to the surface morphology and magnetic properties analyses.

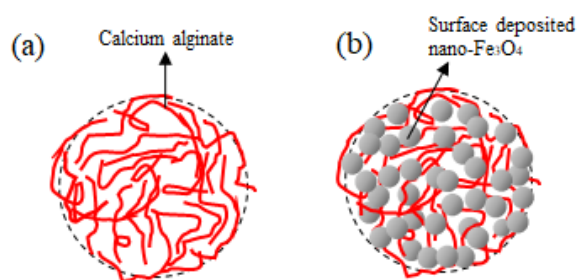


**Fig. 1** Illustration of (a) alginate bead and (b) alginate bead surface deposited with nano-Fe<sub>3</sub>O<sub>4</sub>.

### 2.3 Characterizing the Alginate Beads

Transmission electron microscopy (TEM) and scanning electron microscopy (SEM) analysis were used to characterize the size and shape of nano-Fe<sub>3</sub>O<sub>4</sub> and alginate bead, respectively. Fourier transformed infrared spectroscopy (FTIR) analysis was used to identify the surface functional group of the alginate bead. It was conducted using the ATR technique for the range 400 to 4000 cm<sup>-1</sup>. To determine the

magnetic properties of the beads, magnetic hysteresis loop was generated from vibrating-sample magnetometry (VSM) analysis.

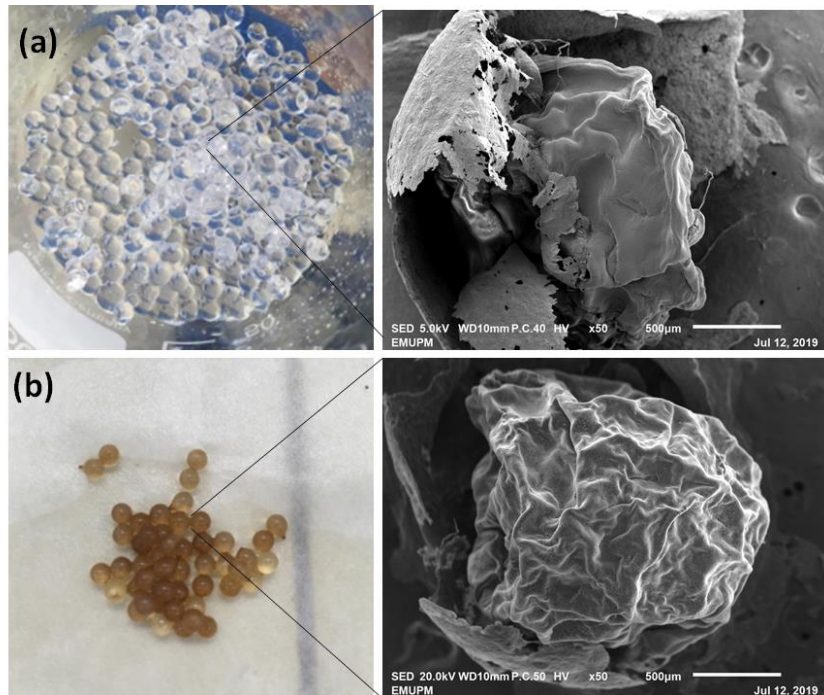


**Fig. 2** Physical outlook of (a) pure alginate bead and (b) nano-Fe<sub>3</sub>O<sub>4</sub> deposited alginate bead [The beads shrank upon dehydration in SEM sample preparation].

### 3 Results and Discussion

TEM analysis on the nano-Fe<sub>3</sub>O<sub>4</sub> clearly showed that this particle is of uniform (spherical) shape (Fig. 3). The average particle size is  $30.8 \pm 8.2$  nm, as reported in our previous work [3]. Severe agglomeration observed in this image can be ascribed to the overwhelm of interparticle attraction forces over repulsion forces between the bare nanoparticles [16,17]. Meanwhile, there are possibility that the seen agglomeration was induced by the drying step during TEM sample preparation [17,18]. Hence, sonication was imposed on the nano-Fe<sub>3</sub>O<sub>4</sub> (to reduce the agglomeration) before being deposited onto the alginate bead.

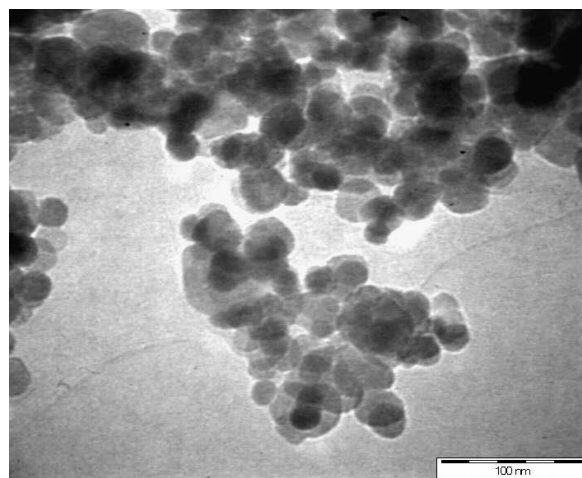


**Fig. 3** TEM image of Fe<sub>3</sub>O<sub>4</sub> nanoparticle.

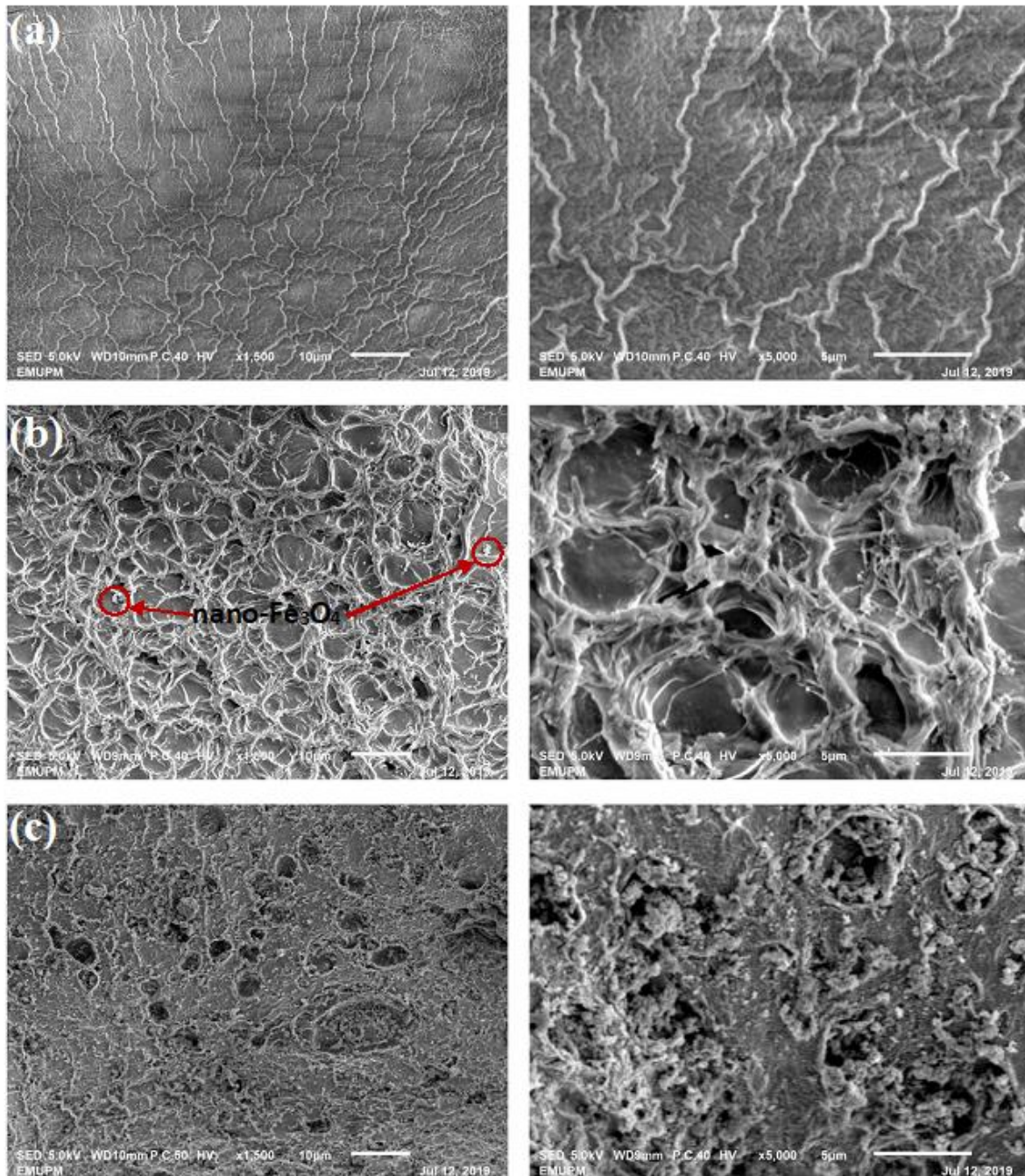


**Fig. 4** SEM images of alginate beads obtained at 1.5k (left) and 5k (right) magnifications. The alginate bead was surface deposited with (a) none, (b) 0.25 g/L, and (c) 3.0 g/L nano-Fe<sub>3</sub>O<sub>4</sub> particles.

In order to identify the change in surface morphology of the bead, SEM analysis was conducted on the alginate bead which was surface deposited with (a) none, (b) 0.25 g/L, and (c) 3.0 g/L nano-Fe<sub>3</sub>O<sub>4</sub> particles. As shown in Fig. 4a, the pure alginate bead displayed a rather smooth texture. On the other hand, the external surface of the nano-Fe<sub>3</sub>O<sub>4</sub> deposited alginate beads appeared to be highly porous. The presence of pores on the bead surface is obviously seen, especially, for the 0.25 g/L nano-Fe<sub>3</sub>O<sub>4</sub> deposited bead (Fig. 4b). Small quantity of Fe<sub>3</sub>O<sub>4</sub> clusters were found to deposit within the pores. In most likelihood, these pores were formed due the sonication step that imposed onto the alginate bead during it mixing with nano-Fe<sub>3</sub>O<sub>4</sub>. The intense sonication imposed high shearing impact that disrupts

the surface of a material until pore is formed [19,20]. In fact, in our previous work, we did not observe such pores on the external surface of alginate beads that were formed without sonication [21]. The formed pores serve as the site to accommodate more  $\text{Fe}_3\text{O}_4$  nanoparticles. In this regard, it was found that the pores on the bead surface were almost fully covered by nano- $\text{Fe}_3\text{O}_4$  when the concentration of nanoparticles being increased to 3.0 g/L (Fig. 4c).

This observation indicates that it is possible to apply sonication as a *pre-treatment* strategy to increase the surface area of an alginate bead. Future work can be done to evaluate the effect of sonication frequency and sonication duration on the pore formation, and thus, the amount of nanoparticles that can be upheld by the pores.

Surface properties of the alginate bead and nano- $\text{Fe}_3\text{O}_4$  deposited alginate bead were identified using FTIR analyser. Fig. 5 shows the FTIR profile of both types of beads. The profile of alginate bead clearly shows that hydroxyl groups are present ( $3264\text{ cm}^{-1}$ ); meanwhile, the peaks at  $1602\text{ cm}^{-1}$  and  $1417\text{ cm}^{-1}$  are ascribed to the asymmetrical and symmetrical stretching vibrations of carboxyl group, respectively [22]. As can be seen from Fig. 5, the nano- $\text{Fe}_3\text{O}_4$  deposited alginate bead has a similar FTIR profile to the pure alginate bead. A peak at around  $579\text{ cm}^{-1} - 632\text{ cm}^{-1}$ , which supposed to be induced by Fe-O vibrations [23,24], was not observed here. Such phenomenon might be due to Fe-O band was covered by another broad peak of the alginate. Otherwise, it was undetectable in the fingerprint region ( $<1000\text{ cm}^{-1}$ ) owing to the concentration of that band was too low.

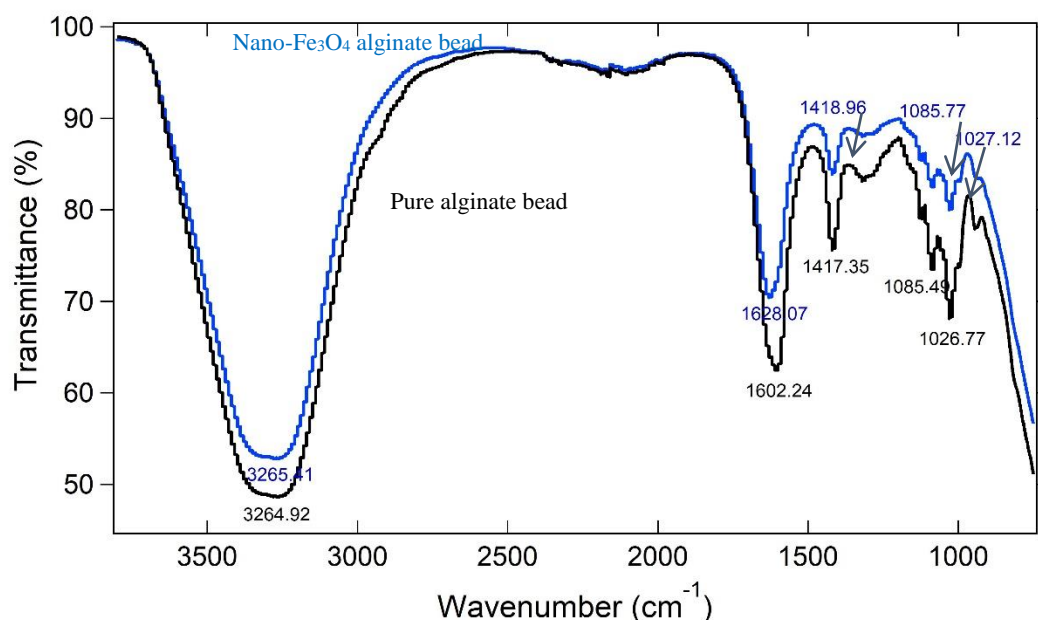


**Fig. 5** FTIR spectra of alginate bead without (black line) and with  $\text{Fe}_3\text{O}_4$  deposition (blue line).

Fig. 6 delineates the hysteresis loop obtained from VSM measurement. As shown in Fig. 6, the saturation magnetization value of the beads which were surface deposited with 0.25 g/L and 3 g/L nano- $\text{Fe}_3\text{O}_4$  were 0.0271 and 0.1198 emu/g, correspondingly; also, the alginate beads possess mild retentivity ( $M_r$ ) of 0.0025 emu/g and 0.0208 emu/g, respectively (Fig. 6). The former indicates that the alginate bead is more magnetically responsive with the increase amount of nano- $\text{Fe}_3\text{O}_4$  loading; while the latter indicates that the magnetic alginate beads were not of perfect superparamagnetic because they retain magnetic memory in zero field.

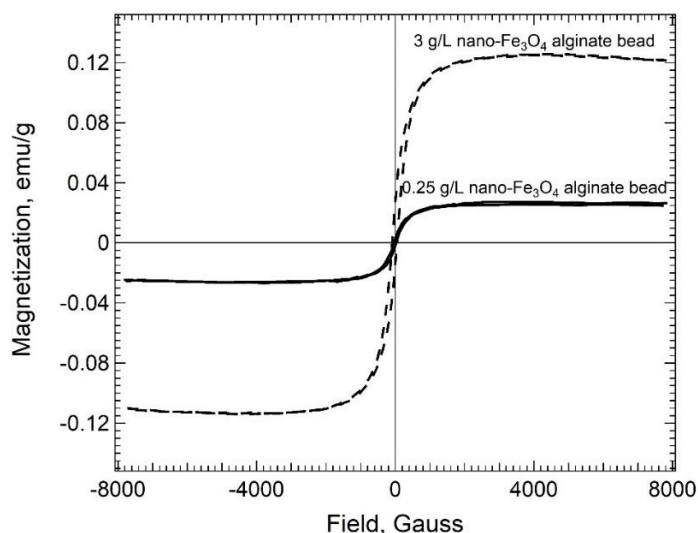


**Fig. 6** Magnetic hysteresis loop of alginate bead surface deposited with different amounts of nano- $\text{Fe}_3\text{O}_4$ .

#### 4 Conclusion

$\text{Fe}_3\text{O}_4$  nanoparticles were successfully deposited onto the external surface of alginate bead. It was found that exposing the alginate bead to an intense sonication may disrupt the surface structure of the bead by creating multiple pores. These surface pores act as a template to hold the  $\text{Fe}_3\text{O}_4$  nanoparticles in place. It was also observed that the bead surface turned rougher upon deposition of  $\text{Fe}_3\text{O}_4$  nanoparticles; this shall offer extra surface area for its potential application in water treatment. Meanwhile, the alginate bead attained net magnetic properties whereby the saturation magnetization value increases with the loading amount of  $\text{Fe}_3\text{O}_4$  nanoparticles. Such magnetic responsiveness suggests that the bead can be re-collected using a magnetic field. Moreover, the cooperative magnetophoresis induced by the attached  $\text{Fe}_3\text{O}_4$  nanoparticle clusters will promote faster magnetic separation than singly dispersed nanoparticles. Future work can be done to evaluate the performance of this magnetic bead in water remediation. Due to the potential concerns of nanosafety, investigation on the potential detachment of nanoparticles from the alginate surface upon exposure to the environmental condition is suggested for future study.

#### Acknowledgement

We sincerely thank the financial support from UCSI University through Pioneer Scientist Incentive Fund (PSIF) with project code Proj-In-FETBE-049.

#### References

- [1] G.N. Hlongwane, P.T. Sekoai, M. Meyyappan, K. Moothi, Simultaneous removal of pollutants from water using nanoparticles: A shift from single pollutant control to multiple pollutant control, *Science of The Total Environment* 656 (2019) 808-833. <https://doi.org/https://doi.org/10.1016/j.scitotenv.2018.11.257>
- [2] F. Pulizzi, W. Sun, Treating water with nano, *Nature Nanotechnology* 13 (2018) 633-633. <https://doi.org/10.1038/s41565-018-0238-4>
- [3] S.P. Yeap, S.S. Leong, A.L. Ahmad, B.S. Ooi, J. Lim, On Size Fractionation of Iron Oxide Nanoclusters by Low Magnetic Field Gradient, *The Journal of Physical Chemistry C* 118 (2014) 24042-24054. <https://doi.org/10.1021/jp504808v>
- [4] J.S. Andreu, J. Camacho, J. Faraudo, M. Benelmekki, C. Rebollo, L.M. Martínez, Simple analytical model for the magnetophoretic separation of superparamagnetic dispersions in a uniform magnetic gradient, *Phys Rev E Stat Nonlin Soft Matter Phys* 84 (2011) 021402. <https://doi.org/10.1103/physreve.84.021402>

- [5] J. Lim, S.P. Yeap, S.C. Low, Challenges associated to magnetic separation of nanomaterials at low field gradient, *Separation and Purification Technology* 123 (2014) 171-174. <https://doi.org/https://doi.org/10.1016/j.seppur.2013.12.038>
- [6] L. Kong, X. Gan, A.L.b. Ahmad, B.H. Hamed, E.R. Evarts, B. Ooi, J. Lim, Design and synthesis of magnetic nanoparticles augmented microcapsule with catalytic and magnetic bifunctionalities for dye removal, *Chemical Engineering Journal* 197 (2012) 350-358. <https://doi.org/https://doi.org/10.1016/j.cej.2012.05.019>
- [7] M. Yegane Badi, A. Azari, H. Pasalari, A. Esrafil, M. Farzadkia, Modification of activated carbon with magnetic Fe<sub>3</sub>O<sub>4</sub> nanoparticle composite for removal of ceftriaxone from aquatic solutions, *Journal of Molecular Liquids* 261 (2018) 146-154. <https://doi.org/https://doi.org/10.1016/j.molliq.2018.04.019>
- [8] K.A. Tan, N. Morad, T.T. Teng, I. Norli, P. Panneerselvam, Removal of Cationic Dye by Magnetic Nanoparticle (Fe<sub>3</sub>O<sub>4</sub>) Impregnated onto Activated Maize Cob Powder and Kinetic Study of Dye Waste Adsorption APCBEE Procedia 1 (2012) 83-89. <https://doi.org/https://doi.org/10.1016/j.apcbee.2012.03.015>
- [9] P. Sun, C. Hui, R. Azim Khan, J. Du, Q. Zhang, Y.-H. Zhao, Efficient removal of crystal violet using Fe<sub>3</sub>O<sub>4</sub>-coated biochar: the role of the Fe<sub>3</sub>O<sub>4</sub> nanoparticles and modeling study their adsorption behavior, *Scientific Reports* 5 (2015). <https://doi.org/10.1038/srep12638>
- [10] C.I. Contescu, S.P. Adhikari, N.C. Gallego, N.D. Evans, B.E. Biss, Activated Carbons Derived from High-Temperature Pyrolysis of Lignocellulosic Biomass. , *Journal of Carbon Research* 4 (2018) 51.
- [11] D. Kibami, C. Pongener, K.S. Rao, D. Sinha, Surface Characterization and Adsorption studies of Bambusa vulgaris-a low cost adsorbent, *Journal of Materials and Environmental Science* 8 (2017) 2494-2505.
- [12] B. Wang, Y. Wan, Y. Zheng, X. Lee, T. Liu, Z. Yu, J. Huang, Y.S. Ok, J. Chen, B. Gao, Alginate-based composites for environmental applications: a critical review, *Critical Reviews in Environmental Science and Technology* 49 (2019) 318-356. <https://doi.org/10.1080/10643389.2018.1547621>
- [13] R. Torres-Caban, C.A. Vega-Olivencia, N. Mina-Camilde, Adsorption of Ni<sup>2+</sup> and Cd<sup>2+</sup> from Water by Calcium Alginate/Spent Coffee Grounds Composite Beads, *Applied Sciences* 9 (2019) 4531.
- [14] J.A.G. Balanay, C.T. Lungu, Morphologic and Surface Characterization of Different Types of Activated Carbon Fibres, *Adsorption Science & Technology* 30 (2012) 355-367. <https://doi.org/10.1260/0263-6174.30.4.355>
- [15] S. Mandal, S.S. Kumar, B. Krishnamoorthy, S.K. Basu, Development and evaluation of calcium alginate beads prepared by sequential and simultaneous methods, *Brazilian Journal of Pharmaceutical Sciences* 46 (2010) 785-793.
- [16] S.P. Yeap, A.L. Ahmad, B.S. Ooi, J. Lim, Electrosteric Stabilization and Its Role in Cooperative Magnetophoresis of Colloidal Magnetic Nanoparticles, *Langmuir* 28 (2012) 14878-14891. <https://doi.org/10.1021/la303169g>
- [17] A. Ali, H. Zafar, M. Zia, I. Ul Haq, A.R. Phull, J.S. Ali, A. Hussain, Synthesis, characterization, applications, and challenges of iron oxide nanoparticles, *Nanotechnol Sci Appl* 9 (2016) 49-67. <https://doi.org/10.2147/nsa.s99986>
- [18] B. Michen, C. Geers, D. Vanhecke, C. Endes, B. Rothen-Rutishauser, S. Balog, A. Petri-Fink, Avoiding drying-artifacts in transmission electron microscopy: Characterizing the size and colloidal state of nanoparticles, *Scientific Reports* 5 (2015) 9793-9793. <https://doi.org/10.1038/srep09793>
- [19] S.K. Low, M.C. Tan, N.L. Chin, Effect of ultrasound pre-treatment on adsorbent in dye adsorption compared with ultrasound simultaneous adsorption, *Ultrasonics Sonochemistry* 48 (2018) 64-70. <https://doi.org/https://doi.org/10.1016/j.ultsonch.2018.05.024>
- [20] M. Tomizawa, F. Shinozaki, Y. Motoyoshi, T. Sugiyama, S. Yamamoto, M. Sueishi, Sonoporation: Gene transfer using ultrasound, *World J Methodol* 3 (2013) 39-44. <https://doi.org/10.5662/wjm.v3.i4.39>
- [21] S.Y. Wai, S.P. Yeap, Z.A. Jawad, Synthesis of magnetite macro-bead for water remediation: process optimization via manipulation of bead size and surface morphology, *IOP Conference Series: Earth and Environmental Science* 463 (2020) 012177. <https://doi.org/10.1088/1755-1315/463/1/012177>
- [22] S. Asadi, S. Eris, S. Azizian, Alginate-Based Hydrogel Beads as a Biocompatible and Efficient Adsorbent for Dye Removal from Aqueous Solutions, *ACS Omega* 3 (2018) 15140-15148. <https://doi.org/10.1021/acsomega.8b02498>
- [23] J. Xu, C. Ju, J. Sheng, F. Wang, Q. Zhang, G. Sun, M. Sun, Synthesis and Characterization of Magnetic Nanoparticles and Its Application in Lipase Immobilization, *Bulletin- Korean Chemical Society* 34 (2013) 2408-2412. <https://doi.org/10.5012/bkcs.2013.34.8.2408>
- [24] S.B. Hammouda, N. Adhoum, L. Monser, Synthesis of magnetic alginate beads based on Fe<sub>3</sub>O<sub>4</sub> nanoparticles for the removal of 3-methylindole from aqueous solution using Fenton process, *Journal of Hazardous Materials* 294 (2015) 128-136. <https://doi.org/https://doi.org/10.1016/j.jhazmat.2015.03.068>